

---

Proceedings of the School Superconductivity and Other Phenomena in Perovskites, Warsaw 2004

## Structure and Transport Properties of $\text{La}_{0.75-x}\text{RE}_x\text{Ca}_{0.25}\text{MnO}_3$ (RE = Gd, Dy, Ho; $0 \leq x \leq 0.75$ ) Manganites

V. DROZD<sup>a</sup>, M. PEKALA<sup>b,\*</sup>, J. KOVAC<sup>c</sup>, I. SKORVANEK<sup>c</sup>,  
M. SZYMAŃSKI<sup>d</sup> AND S. NEDILKO<sup>a</sup>

<sup>a</sup>Department of Chemistry, Kiev State University, Ukraine

<sup>b</sup>Department of Chemistry, Warsaw University

Pasteura 1, 02-093 Warsaw, Poland

<sup>c</sup>Institute of Experimental Physics, SAS, Kosice, Slovakia

<sup>d</sup>Institute of Experimental Physics, Warsaw University, Poland

Structure and transport properties have been studied for a series of  $\text{La}_{0.75-x}\text{RE}_x\text{Ca}_{0.25}\text{MnO}_3$  manganites with heavy rare earth ions of Gd, Dy, Ho substituting La with  $x = 0, 0.10, 0.25, 0.50,$  and  $0.75$ . Polycrystalline samples were prepared by the carbonate precipitation route. The oxygen content was determined by the iodometric titration. The X-ray investigations carried out by the powder method show that the unit cell volume gradually decreases and orthorhombic distortion of the lattice increases with rising RE content. Below the room temperature the electrical resistivity is of the semiconducting type for all the samples studied. Electrical resistivity vs. temperature dependences were analyzed within different models: simple thermal activation, Mott's variable range hopping, adiabatic, nonadiabatic, and bipolaron. The Curie temperatures of Gd, Dy, and Ho substituted manganites determined from magnetization measurements show that at 280 K all the samples are in the paramagnetic phase. The increasing RE fraction reduces magnetization at 4 K as compared to  $\text{La}_{0.75}\text{Ca}_{0.25}\text{MnO}_3$ .

PACS numbers: 75.47.Lx, 71.38.-k, 72.20.Ee, 75.50.Dd

### 1. Introduction

Transport and magnetic properties of the manganese perovskites showing colossal magnetoresistance (CMR) effect are governed mainly by two factors: the

---

\*corresponding author

hole carrier density and the overlapping of manganese and oxygen orbitals. The hole carrier density is connected with the tetravalent manganese concentration while the overlapping of manganese and oxygen orbitals depends strongly on the Mn–O–Mn bond angle, and thus, it is affected by the A cation average size,  $\langle r_A \rangle$  (the smaller the A cation, the smaller the Mn–O–Mn bond angle). Several authors have reported on the substitution of La for heavier rare-earths in  $\text{La}_{1-x}\text{Ca}_x\text{MnO}_3$  (LCM) [1–4] (RE = Gd), [5, 6] (RE = Dy), [7] (RE = Ho), and [8] (RE = Tb). All these studies were done for the LCM with calcium concentration  $x = 1/3$ . Hwang *et al.* [9] studied the dependence of Curie temperature,  $T_C$ , on tolerance factor,  $t$ , for  $(\text{La}_{1-x}\text{RE}_x)_{0.7}\text{Ca}_{0.3}\text{MnO}_3$  with RE = Pr and Y. They found that the ferromagnetic transition temperature and conductivity decrease very quickly with increasing  $x$ . Electronic and magnetic  $T_C$  vs.  $t$  phase diagram constructed by Hwang *et al.* for  $\text{La}_{0.7}\text{Ca}_{0.3}\text{MnO}_3$  substituted manganites with Pr and Y was confirmed and extended for other rare-earth dopants having smaller than  $\text{La}^{3+}$  ionic radii. Besides ferromagnetic metal and paramagnetic insulator range, this phase diagram contains a spin-glass insulator phase at low temperatures and  $t$  below a critical value for RE = Gd [4] and Dy [6] and Tb [9]. The present paper reports on specific preparation method, structure and transport properties of  $(\text{La}_{1-x}\text{RE}_x)_{0.75}\text{Ca}_{0.25}\text{MnO}_3$  manganites in a paramagnetic range.

## 2. Synthesis

Three series of manganites  $\text{La}_{0.75-x}\text{RE}_x\text{Ca}_{0.25}\text{MnO}_3$  (RE = Gd, Dy, Ho,  $x = 0, 0.25, 0.50, 0.75$ ) were synthesized via carbonates precursor method. Ammonium carbonate,  $(\text{NH}_4)_2\text{CO}_3$ , was used as a precipitator. Aqueous solutions (with concentrations about 0.2 M) of  $\text{La}(\text{NO}_3)_3$ ,  $\text{RE}(\text{NO}_3)_3$ ,  $\text{Ca}(\text{NO}_3)_2$ , and  $\text{Mn}(\text{NO}_3)_2$  were chosen as starting reagents. Their concentrations were determined by trilonometric titration. Ammonium carbonate with 15% excess (in the molar ratio to the sum of the moles of cations in the solution) was slowly added to the appropriately mixed solutions of the metal nitrates. The precipitates were held during 24 hours under the mother solution, then filtrated and rinsed sequentially by a distilled water and ethanol. The powders obtained were dried in air at 80°C.

Carbonate precipitates were converted to  $\text{La}_{0.75-x}\text{RE}_x\text{Ca}_{0.25}\text{MnO}_{3-\delta}$  solid solutions by slowly heating in the air atmosphere up to 810°C with the subsequent annealing at this temperature for several hours. Then the powders were grinded in an agate mortar and annealed at 900°C for 24 hours. Finally, they were grinded again, pressed into pellets and annealed at 1250°C for 48 h in a flowing oxygen atmosphere.

## 3. Measurements

The oxygen content of the  $\text{La}_{0.75-x}\text{RE}_x\text{Ca}_{0.25}\text{MnO}_{3-\delta}$  samples was determined by the iodometric titration assuming that the samples have initial cation

stoichiometry. The X-ray investigations were carried out by the powder method using the diffractometer DRON-3 (Cu  $K_\alpha$  radiation).

Electrical resistivity of bulk samples was measured by a four-probe method with the electric current up to 10 mA. Temperature of the samples located in a closed cycle refrigerator was controlled with an accuracy better than 0.02 K. Magnetization was measured by vibrating sample magnetometer (VSM) equipped with a superconducting coil at a magnetic field of 6 T in a temperature range from 4.2 to 300 K.

#### 4. Structural characterization

The  $ABO_3$  cubic perovskite structure consists of a  $BO_6$  array of corner-shared octahedral with a large cation A at the body-centered position. Geometric stability of the perovskite structure is determined by the Goldschmidt tolerance factor  $t$ . As CMR manganese perovskites have the tolerance factor  $t < 1$ , the structure adjusts to these  $t$  by a cooperative tilting of the corner-shared octahedral leading to the formation of the so-called O-type orthorhombic structure with  $a \leq c/\sqrt{2} \leq b$ . Another distortion of the cubic structure, which is common among manganese perovskites, is caused by Jahn–Teller character of  $Mn^{3+}$  ions at the octahedral sites. This distortion modifies the unit cell in such a way that  $c/\sqrt{2} \leq a \leq b$ .

The tolerance factor for the compositions studied in the present work was calculated by the following formula:

$$t = \frac{(\langle r_A \rangle + r_0)}{\sqrt{2}(\langle r_B \rangle + r_0)},$$

where  $\langle r_A \rangle$ ,  $\langle r_B \rangle$  are the weighted mean ionic radii of cations at the A and B positions of the perovskite  $ABO_3$  structure, respectively. The ionic radii of A were used in nine-fold coordination according to Shannon [10]. The substitution of  $La^{3+}$  ions by  $RE^{3+}$  leads to a reduction of the tolerance factor due to the decrease in the mean ionic ratio  $\langle r_A \rangle$  (see Table I). The tolerance factor  $t'$  is calculated taking into account the  $Mn^{3+}/Mn^{4+}$  ratio determined by the iodometric titration.

X-ray diffraction (XRD) analysis showed that materials are single-phase in all cases. All the compositions obtained had an orthorhombic crystal structure of O- or O'-type depending on the RE content. The results of XRD investigations are summarized in Table I. The orthorhombic distortion of the ideal perovskite structure,  $D$ , which is also shown in Table I, was calculated by the following formula:

$$D = \frac{1}{3} \sum_{i=1}^3 \left| \frac{a_i - \bar{a}}{a_1} \right| \cdot 100,$$

where  $a_1 = a$ ,  $a_2 = b$ ,  $a_3 = c/\sqrt{2}$  and  $\bar{a} = (a \cdot b \cdot c/\sqrt{2})^{1/3}$ .

TABLE I

Crystal lattice parameters and oxygen stoichiometry for the  $\text{La}_{0.75-x}\text{RE}_x\text{Ca}_{0.25}\text{MnO}_{3-\delta}$  systems.

$\text{Mn}^{4+}$ [%]	$a$ [Å]	$b$ [Å]	$c$ [Å]	$V$ [Å <sup>3</sup> ]	$D$	$t$	$t'$
$\text{La}_{0.75}\text{Ca}_{0.25}\text{MnO}_{2.994}$							
23.8	5.471(5)	5.480(4)	7.755(5)	232.5(4)	0.09	0.914	0.914
$\text{La}_{0.50}\text{Gd}_{0.25}\text{Ca}_{0.25}\text{MnO}_{2.997}$							
20.4	5.412(6)	5.462(5)	7.668(5)	226.6(6)	0.31	0.905	0.902
$\text{La}_{0.25}\text{Gd}_{0.50}\text{Ca}_{0.25}\text{MnO}_{2.955}$							
16	5.406(3)	5.533(4)	7.602(5)	227.4(4)	1.17	0.895	0.891
$\text{Gd}_{0.75}\text{Ca}_{0.25}\text{MnO}_{2.932}$							
11.4	5.320(3)	5.581(3)	7.489(5)	222.3(4)	2.27	0.886	0.879
$\text{La}_{0.50}\text{Dy}_{0.25}\text{Ca}_{0.25}\text{MnO}_{2.973}$							
19.6	5.432(3)	5.475(4)	7.727(9)	229.8(7)	0.31	0.902	0.900
$\text{La}_{0.25}\text{Dy}_{0.50}\text{Ca}_{0.25}\text{MnO}_{2.937}$							
12.4	5.362(2)	5.550(2)	7.560(4)	224.9(3)	1.62	0.890	0.884
$\text{Dy}_{0.75}\text{Ca}_{0.25}\text{MnO}_{2.898}$							
4.6	5.291(2)	5.609(3)	7.447(3)	221.0(3)	2.76	0.879	0.868
$\text{La}_{0.50}\text{Ho}_{0.25}\text{Ca}_{0.25}\text{MnO}_{2.973}$							
19.6	5.450(4)	5.449(9)	7.722(7)	229.3(7)	0.09	0.902	0.899
$\text{La}_{0.25}\text{Ho}_{0.50}\text{Ca}_{0.25}\text{MnO}_{2.938}$							
12.6	5.335(5)	5.538(3)	7.556(6)	223.2(5)	1.65	0.889	0.883
$\text{Ho}_{0.75}\text{Ca}_{0.25}\text{MnO}_{2.898}$							
4.6	5.267(3)	5.621(2)	7.417(4)	219.6(3)	3.06	0.876	0.867

One can notice that the crystal lattice parameters  $a$  and  $c$  as well as the unit cell volume decrease with an increase in RE concentration in  $\text{La}_{0.75-x}\text{RE}_x\text{Ca}_{0.25}\text{MnO}_3$ . The parameter  $b$  growth causes the increase of orthorhombic deformation of the unit cell. Similar behavior of the lattice parameters was observed by Ibarra et al. [11] for  $(\text{La}_{1-x}\text{Tb}_x)_{2/3}\text{Ca}_{1/3}\text{MnO}_3$  system.

Most of the authors cited in the present work assume that the  $\text{La}_{0.7-x}\text{RE}_x\text{Ca}_{0.3}\text{MnO}_3$  are oxygen stoichiometric compounds and the only effect of RE substitution for La is a distortion of the crystal structure. Therefore, the hole carrier density, which is determined by the  $\text{Mn}^{3+}/\text{Mn}^{4+}$  ratio, should be fixed. In order to check this statement the total oxygen content and  $\text{Mn}^{4+}$  concentration are shown in Table I. It is notable that  $\text{Mn}^{4+}$  concentration decreases with RE content almost linearly. All samples have the same high temperature treatment history. This can indicate that the oxygen diffusion coefficient in manganites with different RE are different too. High concentration of  $\text{Mn}^{3+}$  ions in the samples with a large  $x$  promotes  $\text{O} \rightarrow \text{O}'$  structural transition and also affects their conductivity.

According to the XRD diffraction data all samples are single-phase but a broadening of the diffraction lines is observed at a higher  $x$ . It may be caused by the increase in melting temperature in  $\text{La}_{0.7-x}\text{RE}_x\text{Ca}_{0.3}\text{MnO}_3$  series. Therefore, higher synthesis temperatures or longer periods of sintering are necessary to reach the equilibrium and the oxygen stoichiometry for the samples with different  $x$ . Another possibility is that La substitution for RE causes some additional disorder in the crystal structure which is compensated by oxygen deficiency increase (or  $\text{Mn}^{4+}$  ions concentration decrease). But if this is true, then there should be a minimum (which was not observed) on oxygen content vs. composition curves for the medium values of  $x$ . Moreover, the  $\text{RE}_{0.75}\text{Ca}_{0.25}\text{MnO}_3$  and  $\text{La}_{0.75}\text{Ca}_{0.25}\text{MnO}_3$  systems should have the same oxygen stoichiometry.

### 5. Transport properties

Below the room temperature all the manganites studied exhibit a temperature variation characteristic of semiconducting solids. Electrical resistivity at 280 K ranges between 5 and 300  $\text{m}\Omega\cdot\text{m}$  for the Gd-, Dy-, and Ho-based series, as shown in Table II. Since the electrical resistivity raises rapidly while reducing temperature below 150 to 100 K, the measurements at the lowest temperature could not be performed. The values of activation energy listed in Table II do not exceed 170 meV for the highest RE content and diminish slowly below 140 meV at  $x = 0.25$ , almost independent of RE atom.

The Curie temperatures of Gd, Dy, and Ho substituted manganites determined from magnetization measurements show that at 280 K all the samples are in the paramagnetic phase (Table II). The increasing RE fraction reduces magnetization at 4 K as compared to  $\text{La}_{0.75}\text{Ca}_{0.25}\text{MnO}_3$ . This influence is the strongest for Gd. Table II shows that the absolute values of electrical resistivity at 280 K remarkably diminish when the RE content varies from 0.75 down to 0.25. Such a tendency may be related to the reduced structural disorder and/or to reduced magnetic scattering of electrons, when RE content decreases.

There is a variety of approaches applied to resemble electrical resistivity of magneto-resistive manganites, including a simple thermal activation, Mott's variable range hopping (VRH), adiabatic, nonadiabatic, and bipolaron models. The measured temperature variation of electrical resistivity were carefully fitted to the following formulae of these models:

$$\rho_{AC} = \rho_0 \exp(E_A/kT), \quad \text{thermal activation}, \quad (1)$$

$$\rho_A = A T \exp(E_A/kT), \quad \text{adiabatic polaron}, \quad (2)$$

$$\rho_B = A T^{1/2} \exp(E_A/kT), \quad \text{bipolaron}, \quad (3)$$

$$\rho_N = B T^{3/2} \exp(E_A/kT), \quad \text{nonadiabatic polaron}, \quad (4)$$

$$\rho_M = \rho_0 \exp(T_0/T)^{1/4}, \quad \text{variable range hopping}. \quad (5)$$

TABLE II

Magnetic and electrical parameters for  $\text{La}_{0.75-x}\text{RE}_x\text{Ca}_{0.25}\text{MnO}_3$  systems.

Magnetization at 4 K at 3T [A m <sup>2</sup> /kg]	Curie temperature [K]	Resistivity at 280 K [mΩ·m]	Activation energy [meV]	$T_0$ (VRH) 10 <sup>8</sup> K
$\text{Gd}_{0.75}\text{Ca}_{0.25}\text{MnO}_{2.932}$				
32	260	79.2	166	4.9
$\text{La}_{0.25}\text{Gd}_{0.50}\text{Ca}_{0.25}\text{MnO}_{2.955}$				
54	125	36.8	156	4.2
$\text{La}_{0.50}\text{Gd}_{0.25}\text{Ca}_{0.25}\text{MnO}_{2.997}$				
91	91	5.9	137	2.4
$\text{Dy}_{0.75}\text{Ca}_{0.25}\text{MnO}_{2.898}$				
60	–	300	161	3.8
$\text{La}_{0.25}\text{Dy}_{0.50}\text{Ca}_{0.25}\text{MnO}_{2.937}$				
		35.2	159	3.7
$\text{La}_{0.50}\text{Dy}_{0.25}\text{Ca}_{0.25}\text{MnO}_{2.973}$				
		7.8	137	3.7
$\text{Ho}_{0.50}\text{Ca}_{0.25}\text{MnO}_{2.938}$				
70	–	480	157	5.1
$\text{La}_{0.25}\text{Ho}_{0.50}\text{Ca}_{0.25}\text{MnO}_{2.938}$				
		53.8	156	4.1
$\text{La}_{0.50}\text{Ho}_{0.25}\text{Ca}_{0.25}\text{MnO}_{2.973}$				
		33.0	139	2.9
$\text{La}_{0.75}\text{Ca}_{0.25}\text{MnO}_{2.994}$				
97	244	4.5	109	0.73

In Fig. 1 the resistivity data are plotted in coordinates proper to the models tested. The derived values of the correlation coefficient “ $R$ ” for the RE substituted are relatively lower for VRH model. However, the extracted values of  $T_0$  parameter for Mott’s formula lie in a reasonable range, as compared to similar systems [7]. The values of  $R$  do not differ significantly when comparing the simple thermal activation model and the three different polaron ones. Thus, it is not possible to select the unambiguous model describing the present data.

The relatively poor electrical resistivity for the substituted  $\text{La}_{0.75-x}\text{RE}_x\text{Ca}_{0.25}\text{MnO}_3$  manganites seems to be related to the remarkable difference between the ionic radii of La and Gd, Dy and Ho ions. This in turn increases a buckling of  $\text{MnO}_6$  octahedra and reduces the electron transport between  $\text{Mn}^{3+}$  and  $\text{Mn}^{4+}$  sites, as it was also reported for Dy substituted  $\text{La}_{0.7-x}\text{RE}_x\text{Ca}_{0.3}\text{MnO}_3$  [5] and Gd substituted  $\text{La}_{0.7-x}\text{RE}_x\text{Sr}_{0.3}\text{MnO}_3$  [12].

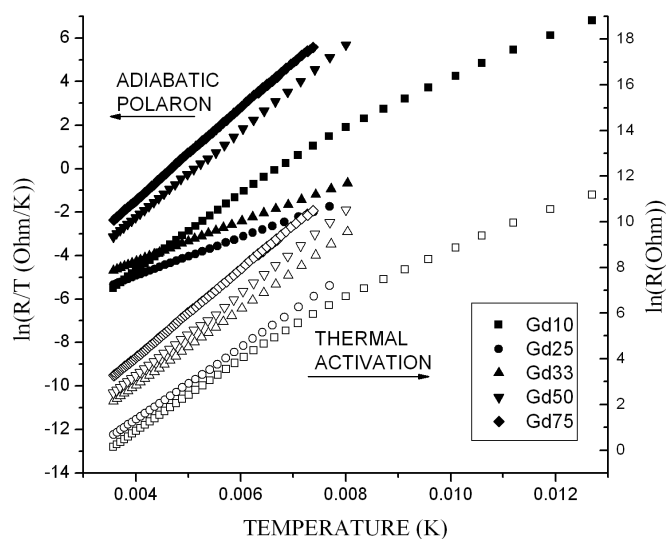


Fig. 1. Fits of  $R(T)$  curves for  $La_{0.7-x}Gd_xCa_{0.3}MnO_3$  to thermal activation (open symbols) and adiabatic polaron (solid symbols) models.

### Acknowledgments

One of the authors (V.D.) thanks the Mianowski Fund-Foundation for the Promotion of Science (Poland) for the support during his stay in Warsaw. The research was also supported in parts by NATO grants (PST.CLG.979446 & PST.MEM.CLG.980654) and SPUB-145.

### References

- [1] E.P. Rivas-Padilla, P.N. Lisboa-Filho, W.A. Ortis, *J. Solid State Chem.* **177**, 1338 (2004).
- [2] L.E. Hueso, P. Sande, F. Rivadulla, A. Fondado, J. Rivas, M.A. López-Quintela, *J. Magn. Magn. Mater.* **242-245**, 665 (2002).
- [3] M. Jaime, H.T. Hardner, M.B. Salamon, M. Rubinstein, P. Dorsey, D. Emin, *Phys. Rev. Lett.* **78**, 951 (1997).
- [4] M. Rubinstein, D.J. Gillespie, J.E. Snyder, T.M. Tritt, *Phys. Rev. B* **56**, 5412 (1997).
- [5] S.M. Yusuf, R. Ganguly, K.R. Chakraborty, P.K. Mishra, S.K. Paranjpe, J.V. Yakhmi, V.C. Sahni, *J. Alloys Compd.* **326**, 89 (2001).
- [6] T. Terai, T. Kakeshita, T. Fukuda, T. Saburi, N. Takamoto, K. Kindo, M. Honda, *Phys. Rev. B* **58**, 14908 (1998).
- [7] V. Ravindranath, M.S. Ramachandra Rao, G. Rangarajan, Yafeng Lu, J. Klein, R. Klingeler, S. Uhlenbruck, B. Büchner, R. Gross, *Phys. Rev B* **63**, 184434 (2001).

- [8] J.M. De Teresa, M.R. Ibarra, J. García, J. Blasco, C. Ritter, P.A. Algarabel, C. Marquina, A. del Moral, *Phys. Rev. Lett.* **76**, 3392 (1996).
- [9] H.Y. Hwang, S.-W. Cheong, P.G. Radaelli, M. Marezio, B. Battlog, *Phys. Rev. Lett.* **75**, 914 (1995).
- [10] R.D. Shannon, *Acta Crystallogr. A* **32**, 751 (1976).
- [11] M.R. Ibarra, J.M. De Teresa, in: *Colossal Magnetoresistance, Charge Ordering and Related Properties of Manganese Oxides*, Eds. C.N.R. Rao, B. Raveau, World Scientific, Singapore 1998, p. 83.
- [12] Y. Sun, M.B. Salamon, W. Tong, Y. Zhang, *Phys. Rev. B* **66**, 094414 (2002).